

Full Paper

Green Synthesis of Nanoscale Nb₂O₅ Particles, their Characterization and use in the Modification of an Electrochemical Sensor

**Ali Sobhani-Nasab,^{1,2} Esmail Sohoul, ^{3,*} Nazila Gholipour,^{4,5} and
Mohammad Hossein Ghanbari^{4,5}**

¹*Social Determinants of Health (SDH) Research Center, Kashan University of Medical Sciences, Kashan, Iran*

²*Core Research Lab, Kashan University of Medical Sciences, Kashan, Iran*

³*Department of Analytical Chemistry, Faculty of Science, Imam Hossein University, Tehran, Iran*

⁴*Chemical Injuries Research Center, Systems Biology and Poisonings Institute, Baqiyatallah University of Medical Sciences, Tehran, Iran*

⁵*Faculty of Pharmacy, Baqiyatallah University of Medical Sciences, Tehran, Iran*

*Corresponding Author, Tel.: +9821770104936; Fax: +982177104940

E-Mail: Esmailshimi@yahoo.com

Received: 15 December 2018 / Received in revised form: 11 March 2019 /

Accepted: 17 March 2019 / Published online: 30 April 2019

Abstract- An alternative green and new method was proposed for preparing Nb₂O₅ nanoparticles (NPs). The nano-sized particles were characterized using FT-IR, XRD, EDX, SEM and VSM techniques. The best sample in terms of dimensions was 50-70 nm in size. In order to investigate its electrochemical application, it was used to detect uric acid and CV, DPV and EIS techniques were applied for this purpose. Detection limit 3 μM was achieved using this method for of uric acid.

Keywords - Nb₂O₅, Nanoparticles, Green Method, electrochemical, uric acid

1. INTRODUCTION

The fabrication of nanosized structures with various size, mono dispersity, and chemical compositions are of great importance in nanotechnology-base fields [1-9]. This stems from the fact that such area could be considered as an alarmingly increasing field which is able to produce materials with very specific features [10-23]. Recently niobium-based components have received much attention. This stems from the fact that such materials, particularly Nb₂O₅, have been employed for their optical, electrical, thermal, electrical, and catalytic (due to having wide band gap value ranging from 1 to 4 eV) features [24,25]. Besides, niobium (V) oxide belongs to those n-type metal transition oxides which are nontoxic, and have great specific surface area and chemical stability. More importantly, they can be considered as a good candidate to be used in high technology industries, where they are being used in microcapacitors, electro-electronic capacitors, and energy storage devices with high energy density [26-30].

Uric acid is one of the most important nitrogen compounds in the urine and is the cause of many clinical disorders. Gout is originated from accumulation of uric acid in the tissues of the body. Moreover, uric acid is also considered as one of the causes of cardiovascular disease. Therefore, determination and measurement of uric acid is important. In this work, the composition of a carbon paste used for preparing an was improved using the Nb₂O₅ nanoparticles. The resulting modified carbon paste electrode (CPE) was used for detection of uric acid using various electrochemical techniques.

2. EXPERIMENTAL

2.1. Synthesis of Nb₂O₅ nanoparticles

Nowadays, researchers have synthesis various nanomaterial by novel and simple methods [31-47]. Analytical grade reagents were used for preparing Nb₂O₅ nanostructures, without any prior treatments. These nanoparticles were prepared through sequential method. At first, 1 mmol of niobium (V) chloride was dissolved in deionized water (30 mL) to obtain solution A. In parallel a solution of 3 mL of the capping agent in 40 mL of deionized water (Solution B) was prepared and then solution A was added to solution B under stirring. The solid product was isolated through centrifugation, and repeatedly washed with ethyl alcohol and water, and eventually dried at 70 °C in air atmosphere and then sintered at 700 °C for 30 min.

2.2. Reagents and apparatus

A Philips powder X-ray diffractometer (X'PertPro, Cu K α 1 (λ =1.54 Å), at 40 kV and 30 mA was used to record the X-ray diffraction (XRD) patterns of the samples in the window of $10^{\circ} \leq 2\theta \leq 70^{\circ}$ at a 0.02° step. Field emission scanning electron microscopy (FESEM) studies

were performed using a Tescan Mira3 instrument. (FESEM). Transmission electron microscopy (TEM) studies were conducted using a JEM-2100 instrument at an acceleration voltage of 200 kV). A Shimadzu UV–Vis scanning UV–Vis diffuse reflectance spectrometer, was used for UV–Vis spectroscopy analyses A Philips XL30 microscope was used for the energy dispersive spectrometry (EDS). and the the vibrating sample magnetometry (VSM) analyses were performed on a Meghnatis Daghigh Kavir Co instrument in a magnetic field window of of $\pm 10,000$ Oe, at ambient temperature. Fourier transform infrared (FT-IR) spectra were obtained using a Magna-IR 550 Nicolet spectrometer with a 0.125 cm^{-1} resolution. The tests were performed using KBr pellets ($400\text{--}4000\text{ cm}^{-1}$).

2.3. Preparation of the electrode

0.13 g graphite is mixed with 0.01 g of Nb_2O_5 NPs as a modifier ($\text{Nb}_2\text{O}_5\text{NPs/CPE}$) and then several drops (0.06 g) of paraffin and 1 mL acetone was added to this mixture. After mixing for several minutes, the mixture is then moved to an oven at $50\text{ }^\circ\text{C}$ and for removing acetone. Then, the composite mixture was used to fill a part of a polyethylene tube (3.0 mm). For the electrical connection of the carbon paste to an electrochemical device, a copper wire connected to the paste located in the inner cavity of the plastic syringe was used. The bare CPE was also obtained by combining 0.14 g graphite and 0.06 g oil.

3. RESULT

The XRD pattern of the Nb_2O_5 nanoparticles prepared using 20 as the capping agent at temperature $700\text{ }^\circ\text{C}$ (Fig. 1) shows that the Nb_2O_5 nanoparticles have a pure phase with high crystallinity was formed. The XRD signals are all located at 22.53° ((112) line), 28.22° ((002) line), and 36.24° ((200) line), which correspond to the Orthorhombic Nb_2O_5 with space group Pbam (JCPDS card file no. 27-1003) and $a=6.1680\text{ \AA}$ $b=29.3120\text{ \AA}$ and $c=3.9360\text{ \AA}$ as the cell parameters. The mean crystallite size of the Nb_2O_5 nanoparticles estimated by the Scherrer formula is 20 nm.

The purity and chemical composition of the Nb_2O_5 nanoparticles were passed through EDS, and it can be seen in the results (Fig. 2) that the Nb_2O_5 nanoparticles consisted of two different elements such as, Nb, and O. Moreover, no impurity peaks were seen. This suggests that as-prepared Nb_2O_5 nanoparticles have high purity.

We used the SEM technique to investigate the shape of Nb_2O_5 nanoparticles. Based on Fig. 3, one can simply find out that synthesized Nb_2O_5 nanoparticles have sphere-like morphology which their particle size are approximately 50–70 nm.

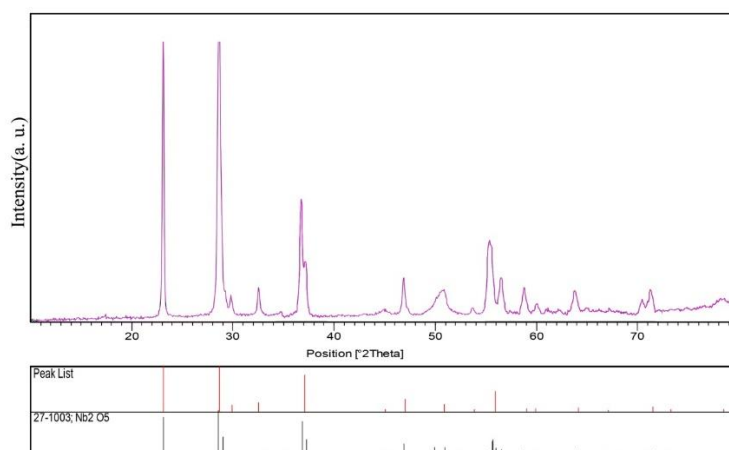


Fig. 1. XRD pattern recorded for the Nb₂O₅ sample prepared using Tween (calcined at 700 °C)

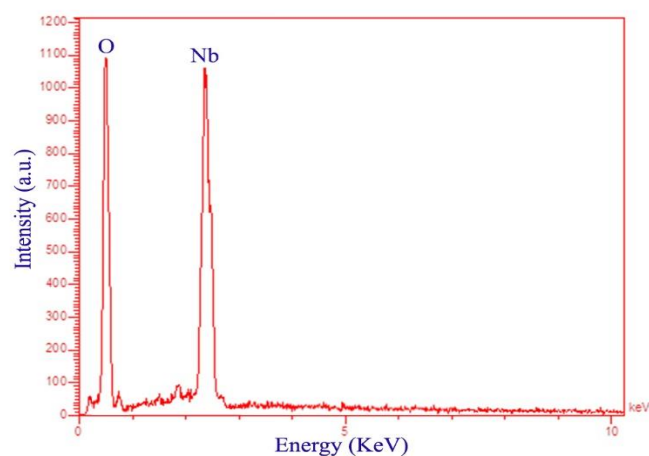


Fig. 2. EDS pattern of Nb₂O₅ nanoparticles in present Tween calcined at 700 °C

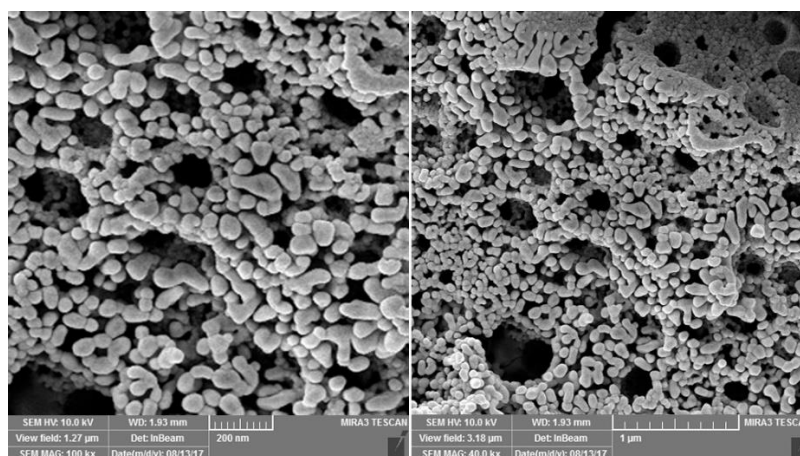


Fig. 3. SEM recorded for Nb₂O₅ prepared using Tween (calcined at 700 °C)

Fig. 4 shows the infrared spectra of the as-fabricated powders in presence of tween and calcinations at 700 °C. According to FT-IR spectra, the weak absorption band positioned at 3443 cm^{-1} can be related to stretching vibration of the O-H band of H_2O molecules which was absorbed on the surface of the nanoparticles. There are some peaks that could be assigned with the presence of tween such as 1430 cm^{-1} . The characterization peaks in the Nb_2O_5 nanoparticles spectrum are 539 cm^{-1} (vibration of atoms in tetrahedral oxygen environment; Nb–O) [45].

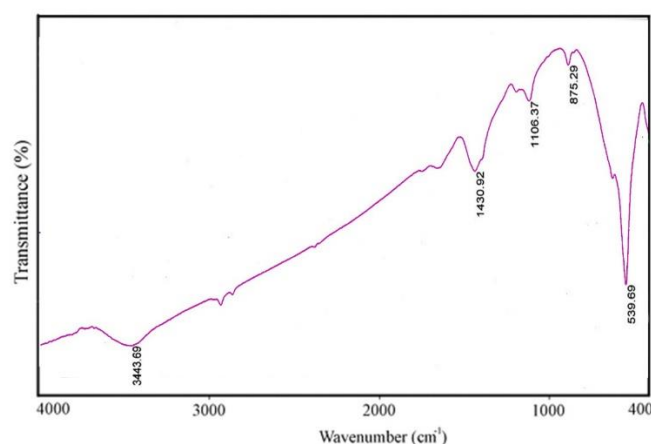


Fig. 4. FT-IR spectra of Nb_2O_5 nanoparticles in present Tween calcined at 700 °C

3.1. Electrochemical behavior of electrodes

Given the excellent performance of different nanomaterials in electrochemistry, many electrochemical scientists have focused on this field [46-53]. Using a 5 mM solution of $\text{K}_3\text{Fe}(\text{CN})_6/\text{K}_4\text{Fe}(\text{CN})_6$ in 0.1 M KCl solution, the electrochemical behaviors of unmodified CPE and Nb_2O_5 NPs/CPE were monitored.

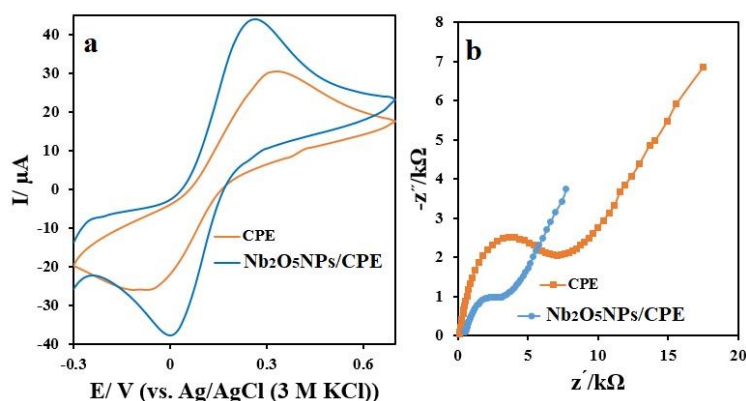


Fig. 5. a) CVs obtained for a 5 mM solution of $\text{K}_3\text{Fe}(\text{CN})_6/\text{K}_4\text{Fe}(\text{CN})_6$ in 0.1 M KCl using an unmodified CPE and an Nb_2O_5 NPs/CPE, b) The Nyquist diagram based on the EIS measurements performed under the same conditions

A comparison of the two electrodes is presented in Fig. 5a. As is evident, ΔE for $K_3Fe(CN)_6/K_4Fe(CN)_6$ at the CPE and Nb_2O_5NPs/CPE surfaces are 34 mV and 21 mV, respectively. Moreover, Nyquist plots of electrodes is presented in Fig. 5b which shows that the electron transfer resistance of Nb_2O_5NPs/CPE is less than the CPE indicating the catalytic activity of nanoparticles.

3.2. Analysis of uric acid

The results of the analyses of a uric acid sample using an unmodified CPE and Nb_2O_5NPs/CPE are illustrated in Fig. 6. As can be seen the a 50 μM solution of uric acid at the Nb_2O_5NPs/CPE surface has a higher oxidation current relative to CPE surface (at potential of 0.27 V and in a phosphate buffer (PBS) (pH=7; scan rate=100 mV/s.) It is seen that the modified electrode response for uric acid is appropriate and this electrode can be used to detect trace concentrations of uric acid.

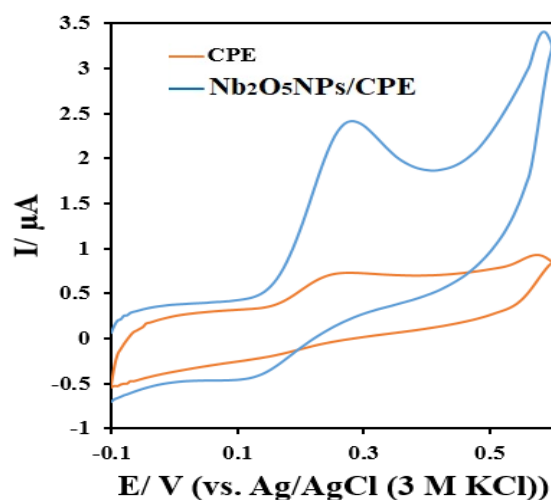


Fig. 6. CVs of the CPE and Nb_2O_5NPs/CPE in PBS (pH=7) at 100 mV/s for 50 μM uric acid

To evaluate the role of changing the scan rate on the electro-oxidation of the analyte at Nb_2O_5NPs/CPE , cyclic voltammetry analyses were performed at different scan rates in the window of 10 to 400 $mV s^{-1}$ (Fig. 7). Moreover, the plot of current versus squared scan rate indicates that the electro oxidation of uric acid in PBS, using the modified electrode is diffusion-controlled.

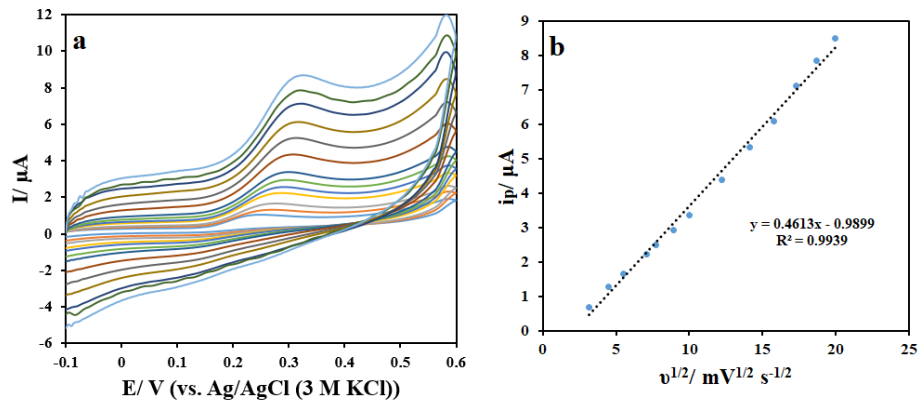


Fig. 7. a) CVs of 50 μM uric acid in 0.1 M PBS, pH=7.0 at various scan rates. b) I_p vs. $v^{1/2}$

3.3. Effect of analyte concentration

The effect of different concentrations on the peak current was investigated using DPV technique. Fig. 8a shows corresponding voltammograms of various concentrations of uric acid in PBS (pH=7). The calibration curve is also shown in Fig. 8b for the concentration range of 3 to 100 μM , the detection limit obtained for uric acid from the LOD= S/M ratio is 1.1 μM .

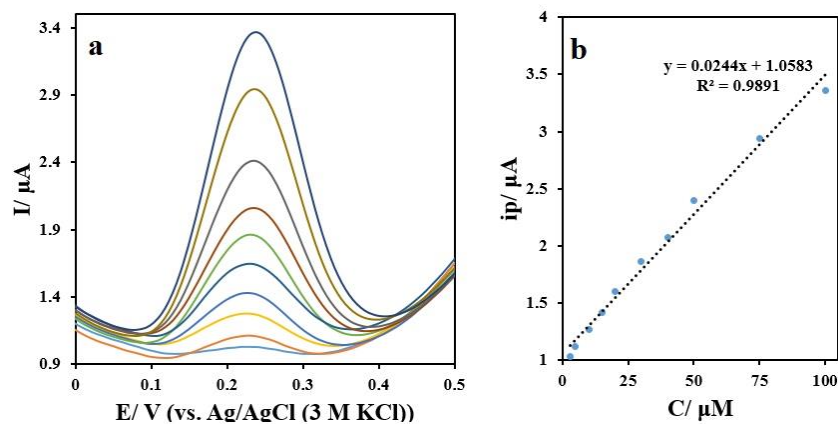


Fig. 8. a) DPVs of 3-100 μM uric acid in 0.1 M PBS (pH=7.0) using $\text{Nb}_2\text{O}_5\text{NPs/CPE}$; b) The peak current/uric acid concentration profile.

4. CONCLUSIONS

An eco-friendly procedure was used for preparing Nb_2O_5 nanoparticles, using Tween as a capping agent. The main advantage of this approach is the ease of its use for producing Nb_2O_5 nanoparticles. Synthesized $\text{Nb}_2\text{O}_5\text{NPs}$ were used to modify the carbon paste electrode and uric acid was detected using this modified electrode in aqueous samples at pH=7. The increase in the current of modified electrode compared to the unmodified electrode and lower charge

transfer resistance relative to the modified electrode indicating the good electrochemical activity of this electrode.

Acknowledgment

Authors are grateful to council of Kashan University of Medical Sciences for providing financial support to undertake this work.

REFERENCES

- [1] F. Ahmadi, M. Rahimi-Nasrabadi, A. Fosooni, and M. Daneshmand. *J. Mater. Sci. Mater. Electron.* 27 (2016) 9514.
- [2] M Aghazadeh, *Mater. Lett.* 211 (2018) 225.
- [3] S. M. Hosseinpour-Mashkani, and A. Sobhani-Nasab, *J. Mater. Sci. Mater. Electron.* 27 (2016) 3240.
- [4] A. Sobhani Nasab, S. Pourmasoud, F. Ahmadi, M. Wysokowski, T. Jesionowski, H. Ehrlich, and M. Rahimi-Nasrabadi, *Mater. Lett.* 238 (2019) 159.
- [5] S. M. Pourmortazavi, Z. Marashianpour, M. Sadeghpour Karimi, and M. Mohammad-Zadeh, *J. Mol. Struct.* 1099 (2015) 232-.
- [6] A. Sobhani-Nasab, M. Rangraz-Jeddy, A. Avanes, and M. Salavati-Niasari, *J. Mater. Sci. Mater. Electron.* 26 (2015) 9552.
- [7] S. S. Hosseinpour-Mashkani, S. S. Hosseinpour-Mashkani, and A. Sobhani-Nasab, *J. Mater. Sci. Mater. Electron.* 26 (2015) 4351.
- [8] A. Sobhani-Nasab, and M. Behpour, *J. Mater. Sci. - Mater. Electron.* 27 (2016) 1191.
- [9] S. M. Pourmortazavi, M. Taghdiri, N. Samimi, and M. Rahimi-Nasrabadi, *Mater. Lett.* 121 (2014) 5.
- [10] M. Rahimi-Nasrabadi, M. Behpour, A. Sobhani-Nasab, and S. M. Hosseinpour-Mashkani, *J. Mater. Sci. Mater. Electron.* 26 (2015) 9776.
- [11] J. Shi, P. Ci, F. Wang, H. Peng, P. Yang, L. Wang, and P. K. Chu, *Electrochim. Acta.* 56 (2011) 4197.
- [12] Y. Bai, J. Wu, X. Qiu, J. Xi, J. Wang, J. Li, and I. Chen, *Appl. Catal. B* 73 (2007) 144.
- [13] M. Rahimi-Nasrabadi, M. Behpour, A. Sobhani-Nasab, and M. Rangraz Jeddy, *J. Mater. Sci. Mater. Electron.* 27 (2016) 11691.
- [14] M. Salavati-Niasari, F. Soofivand, A. Sobhani-Nasab, M. Shakouri-Arani, M. Hamadani, and S. Bagheri, *J. Mater. Sci. Mater. Electron.* 28 (2017) 14965.
- [15] M. Rahimi-Nasrabadi, F. Ahmadi, and M. Eghbali-Arani, *J. Mater. Sci. Mater. Electron.* 27 (2016) 11873.
- [16] S. M. Hosseinpour-Mashkani, A. Sobhani-Nasab, and M. Mehrzad, *J. Mater. Sci. Mater. Electron.* 26 (2015) 5758.

- [17] S. M. Hosseinpour-Mashkani, M. Ramezani, A. Sobhani-Nasab, and M. Esmaeili-Zare, *J. Mater. Sci. Mater. Electron.* 26 (2015) 6086.
- [18] S. M. Hosseinpour-Mashkani, and A. Sobhani-Nasab, *J. Mater. Sci. Mater. Electron.* 26, (2015) 7548.
- [19] M. Rahimi-Nasrabadi, F. Ahmadi, and A. Fosooni, *J. Mater. Sci. Mater. Electron.* 28 (2017) 537.
- [20] V. Umapathy, P. Neeraja, A. Manikandan, and P. Ramu, *Trans. Nonferrous Met.* 27 (2017) 1785.
- [21] A. Alborzi, and S. Khademolhoseini, *J. Mater. Sci. Mater Electron.* 27 (2016) 3963
- [22] A. P. de Moura, L. H. de Oliveira, I. L. Rosa, C. S. Xavier, P. N. Lisboa-Filho, and J. A. Varela, *Sci. World J.* 32 (2015) 476.
- [23] B. Senthilkumar, and R. K. Selvan, *J. Colloid Interface Sci.* 426 (2014) 280.
- [24] R. Brayner, and F. Bozon-Verduraz, *Phys. Chem. Chem. Phys.* 5 (2003) 1457.
- [25] Y. Hong, C. Li, G. Zhang, Y. Meng, B. Yin, Y. Zhao, and W. Shi, *Chem. Eng. J.* 299 (2016) 74.
- [26] M. N. Chong, B. Jin, C. W. K. Chow, and C. Saint, *Water Res.* 44 (2010) 2997.
- [27] Q. Deng, M. Li, J. Wang, K. Jiang, Z. Hu, and J. Chu, *Nanotechnology* 29 (2018) 185401.
- [28] A. A. Ismail, and D. W. Bahnemann, *Sol. Energy Mater. Sol. Cells* 128 (2014) 85.
- [29] S. Sarkar, R. Das, H. Choi, and C. Bhattacharjee, *RSC Adv.* 4 (2014) 57250.
- [30] B. Ohtani, *Electrochemistry* 82 (2014) 414.
- [31] M. Ramezani, S. M. Hosseinpour-Mashkani, A. Sobhani-Nasab, and H. Ghasemi Estarki, *J. Mater. Sci. Mater. Electron.* 26 (2015) 7588.
- [32] M. Ramezani, A. Sobhani-Nasab, and S. M. Hosseinpour-Mashkani, *J. Mater. Sci. Mater. Electron.* 26 (2015) 4848.
- [33] M. Eghbali-Arani, A. Sobhani-Nasab, M. Rahimi-Nasrabadi, and S. Pourmasoud, *J. Mater. Sci. Mater. Electron.* 47 (2018) 3757.
- [34] S. S. Hosseinpour-Mashkani, and A. Sobhani-Nasab *J. Mater. Sci. Mater. Electron.* 28 (2017) 16459.
- [35] M. Rahimi-Nasrabadi, M. Rostami, F. Ahmadi, A. F. Shojaie, and M. D. Rafiee, *J. Mater. Sci. Mater. Electron.* 27 (2016) 11940.
- [36] S. Mostafa Hosseinpour-Mashkani, and A. Sobhani-Nasab, *J. Mater. Sci. Mater. Electron.* 28 (2017) 4345.
- [37] M. Maddahfar, M. Ramezani, M. Sadeghi, and A. Sobhani-Nasab, *J. Mater. Sci. Mater. Electron.* 26 (2015) 7745.
- [38] A. Sobhani-Nasab, and M. Behpour *J. Mater. Sci. Mater Electron.* 27 (2016) 11946.
- [39] S. M. Hosseinpour-Mashkani, M. Maddahfar, and A. Sobhani-Nasab, *J. Electron. Mater.* 45 (2016) 3612.

- [40] F. Ahmadi, M. Rahimi-Nasrabadi, A. Fosooni, and M. Daneshmand, *J. Mater. Sci. Mater. Electron.* 27 (2016) 9514.
- [41] S. M. Asgarian, S. Pourmasoud, Z. Kargar, A. Sobhani-Nasab, and M. Eghbali-Arani, *Mater. Res. Express* 6 (2019) 15023.
- [42] H. Kooshki, AliSobhani-Nasab, M. Eghbali-Arani, F. Ahmadi, V. Ameri, and M. Rahimi-Nasrabadi, *Separat. Purificat. Technol.* (2019) 873.
- [43] M. Salavati-Niasari, F. Soofivand, A. Sobhani-Nasab, M. Shakouri-Arani, and S. Bagheri, *Adv. Powder Technol.* 27 (2016) 2066.
- [44] F. Sedighi, M. Esmaeili-Zare, A. Sobhani-Nasab, and M. Behpour, *J. Mater. Sci. Mater. Electron.* 29 (2018) 13737.
- [45] S. Zarrin, and F. Heshmatpour, *J. Hazard. Mater.* 351, (2018) 147.
- [46] M. Rahimi-Nasrabadi, S. M. Pourmortazavi, M. Aghazadeh, M. R. Ganjali, M. Sadeghpour Karimi, and P. Norouzi, *J. Mater. Sci. Mater. Electron.* 28 (2017) 9478.
- [47] M. Rahimi-Nasrabadi, V. Pourmohamadian, M. Sadeghpour Karimi, H. R. Naderi, M. A. Karimi, K. Didehban, and M. R. Ganjali, *J. Mater. Sci. Mater. Electron.* 28 (2017) 12391.
- [48] B. A. H. Zaidan, E. Sohoul, and S. Mazaheri, *Anal. Bioanal. Electrochem.* 11 (2019) 108.
- [49] M. Rahimi-Nasrabadi, S. M. Pourmortazavi, Z. Rezvani, K. Adib, and M. R. Ganjali, *Mater. Manuf. Processes* 30 (2015) 34.
- [50] J. Hassanzadeh, B. Rezaei Moghadam, A. Sobhani-Nasab, F. Ahmadi, and M. Rahimi-Nasrabadi, *Spectrochim. Acta Part A* 214 (2019) 451.
- [51] A. Khoshroo, L. Hosseinzadeh, A. Sobhani-Nasab, M. Rahimi-Nasrabadi, and H. Ehrlich, *J. Electroanal. Chem.* 823 (2018) 61.
- [52] J. Amani, M. Maleki, A. Khoshroo, A. Sobhani-Nasabb, and M. Rahimi-Nasrabadi, *Anal. Biochem.* 548 (2018) 53.
- [53] M. Rahimi-Nasrabadi, H. R. Naderi, M. Sadeghpour Karimi, F. Ahmadi, and S. M. Pourmortazavi, *J. Mater. Sci. Mater. Electron.* 28 (2017) 1877.